Growth of Bi thin films on quasicrystal surfaces

H. R. Sharma,[1,2,*] V. Fournée,[3] M. Shimoda,[1,4] A. R. Ross,[5] T. A. Lograsso,[5] P. Gille,[6] and A. P. Tsai[1,4,7]
[1]*National Institute for Materials Science, 1-2-1 Sengen, Tsukuba, Ibaraki 305-0047, Japan*
[2]*Department of Physics and Surface Science Research Centre, The University of Liverpool, Liverpool L69 3BX, United Kingdom*
[3]*LSG2M, CNRS-UMR 7584, Ecole des Mines, Parc de Saurupt, 54042 Nancy, France*
[4]*SORST, Japan Science and Technology Agency, Japan*
[5]*Department of Chemistry, Ames Laboratory, Iowa State University, Ames, Iowa 50011, USA*
[6]*Department für Geo- und Umweltwissenschaften, Sektion Kristallographie, Ludwig-Maximilians-Universität München, Theresienstrasse 41, 80333 München, Germany*
[7]*Institute of Interdisciplinary Research for Advanced Materials, Tohoku University, Katahira 2-1-1, 980-8577, Japan*
(Received 12 June 2008; published 14 October 2008)

We present a comprehensive study of Bi thin-film growth on quasicrystal surfaces. The substrates used for the growth are the fivefold surface of icosahedral (*i*)-Al-Cu-Fe and *i*-Al-Pd-Mn and the tenfold surface of decagonal (*d*)-Al-Ni-Co quasicrystals. The growth is investigated at 300 and 525 K substrate temperatures and at different coverage (θ) ranging from submonolayer to ten monolayers. The film is characterized by scanning tunneling microscopy, reflection high-energy electron diffraction, and x-ray photoelectron spectroscopy. At 300 K, the deposited Bi yields a quasicrystalline film for $\theta \leq 1$. For $1 < \theta < 5$, it forms nanocrystallites with (100) surface orientation. The islands have magic heights, which correspond to the stacking of four atomic layers (predominantly). The selection of magic heights is interpreted in terms of quantum size effects arising from the electron confinement within the film thickness. The islands establish rotational epitaxial relationship with the substrate. For higher coverage, the film grows with monatomic height, not with magic heights, and reflects the symmetry of the bulk Bi. When deposition is performed at 525 K, terrace diffusion is more effective, resulting in the aggregation of Bi adatoms developing into a smooth monolayer with quasiperiodic order. At this temperature, multilayers do not adsorb.

DOI: 10.1103/PhysRevB.78.155416 PACS number(s): 61.44.Br, 68.55.−a, 68.37.Ef

I. INTRODUCTION

Quasicrystals are perfectly ordered structures like regular crystals, but they lack periodicity.[1] Their diffraction pattern shows sharp well-defined peaks that often distribute in reciprocal space according to the icosahedral (*i*) or decagonal (*d*) symmetry. These noncrystallographic rotational symmetries are reflected in the growth shape of most single-grain quasicrystals, presenting pentagonal or decagonal facets.[2] Their unique atomic structure correlates with unexpected electronic properties different from those of both amorphous and crystalline alloys.[2] For example, low values of the electrical conductivity σ are typical in Al-based quasicrystals, and σ increases with increasing temperature, contrary to the usual metallic behavior. Their electronic structure is characterized by a minimum in the electronic density of states located at the Fermi level, termed as pseudogap, which is ascribed to both structural and hybridization effects.[3]

The surfaces of quasicrystals have received increasing interest in the past few years, which is motivated in part by their potentially useful properties such as reduced friction and adhesion or corrosion resistance. Developments in the synthesis of large single-grain quasicrystals of high structural quality have opened the possibility to investigate the structure and properties of clean quasicrystalline surfaces in ultrahigh vacuum (UHV) environment. Most studies performed so far have focused on the tenfold surface of the Al-Ni-Co decagonal phase and the fivefold surface of the Al-Pd-Mn and Al-Cu-Fe icosahedral phases. It has been found that under suitable preparation conditions, the surface of quasicrystals are well-ordered two-dimensional (2D) quasiperiodic objects that correspond to perfect truncation of the bulk structure, with no chemical segregation or surface reconstruction, except for some interlayer relaxation (refer to Ref. 4 for recent review).

These progresses have enabled the study of new epitaxial systems: solid-film growth on quasiperiodic substrates. Here the original idea was to use quasicrystals as template to grow another quasiperiodic systems of reduced dimensionality that could not form otherwise. Different observations have shown that some of the symmetry elements of the quasiperiodic substrate are mediated into the film during the growth, either at a mesoscopic scale through the formation of fivefold or tenfold twinning of nanocrystals or at an atomic scale when pseudomorphic growth can be achieved.[4,5] The structure of the film strongly depends on the adsorbate species and the growth mode, which in turn depends on both energetic and kinetic factors. The various observations reported so far in the field of thin-film growth on quasicrystalline surfaces clearly show that it is not possible to predict the film morphology, either smooth 2D or rough three-dimensional (3D) growth, based on thermodynamic relationship between the substrate and adsorbate surface energies and the interfacial energy, because growth occurs far from equilibrium and/or unknown interfacial energy. A more atomistic description of the growth phenomena that would take into accounts both energetic and kinetic factors appears necessary to explain the various observations reported so far.

Franke *et al.*[6] reported the epitaxial growth of either Bi or Sb monolayers on either the tenfold surface of *d*-Al-Ni-Co or the fivefold surface of *i*-Al-Pd-Mn quasicrystals. The depo-

 ©2008 The American Physical Society

sition was performed at 523–573 K temperatures, which are above the multiplayer desorption temperature. The quasiperiodic structure of the deposited Bi or Sb monolayer was demonstrated by low-energy electron diffraction and helium-atom scattering (HAS). Recent *ab initio* studies confirmed the stability of such supported quasiperiodic monolayers and a structure model has been proposed.[7,8]

We recently reported on investigations by scanning tunneling microscopy (STM) and reflection high-energy electron diffraction (RHEED) of a similar system: Bi deposited on the fivefold surface of *i*-Al-Cu-Fe.[9] The Al-Pd-Mn and Al-Cu-Fe icosahedral phases are almost isostructural and their surfaces perpendicular to a fivefold axis are almost identical down to the atomic level,[10] although their chemical compositions in the near surface region are different. The thin-film growth was investigated at room temperature. We observed pseudomorphic growth at submonolayer coverage. At coverage of about five monolayers (MLs), we found the formation of crystalline Bi islands with flat tops and steep edges on top of a Bi wetting layer. The Bi islands have uniform heights, corresponding to four atomic layers or a multiple of this height, which are the so-called "magic heights." Similar phenomena were also observed for Ag thin films grown on the fivefold surface of *i*-Al-Pd-Mn at 365 K.[9] We argued that the driving force for the island height selection is related to quantum size effects (QSEs) induced by the confinement of the electrons within the film thickness in the direction normal to the surface. In such systems, quantum well states develop and their position with respect to the Fermi level depends on the film thickness. Then minimization of the electronic energy favors preferred thickness of the Bi islands.[9] Quantum size effects were later confirmed by Moras *et al.*[11] who directly observed *sp*-derived quantum well states by photoemission spectroscopy in Ag thin films deposited on quasicrystalline templates. It was argued that the confining barrier is mainly driven by the incompatible symmetries of the wave functions at the film substrate interface rather than by the pseudogap in the electronic structure of the substrate.

In this paper, we present extensive studies of Bi thin-film growth observed by various techniques including STM, RHEED, and x-ray photoelectron spectroscopy (XPS). The substrates on which the films are grown include the fivefold surface of both *i*-Al-Pd-Mn and *i*-Al-Cu-Fe as well as the tenfold surface of *d* -Al-Ni-Co. Thin films were grown either at room temperature or at 523 K, a temperature which is above the multilayer desorption temperature. Film thicknesses range from submonolayer coverage up to 10 ML. A wide variety of structures are observed depending on experimental conditions. This includes quasiperiodic Bi wetting layer, formation of nanocrystallites with magic heights, rotational epitaxial relationship between the film and the substrate, and terrace-dependent film morphologies as well.

II. EXPERIMENT

Single-grain icosahedral $Al_{63}Cu_{24}Fe_{13}$ and $Al_{70}Pd_{21}Mn_9$ quasicrystals were cut perpendicular to a fivefold axis. Similarly, single-grain decagonal $Al_{71.7}Ni_{18.7}Co_{9.6}$ quasicrystal was cut perpendicular to the tenfold axis. The surfaces were then mechanically polished using diamond paste down to 0.25 μm. A clean surface was prepared in UHV (base pressure of 1×10^{-10} mbar) by repeated cycles of ion sputtering (Ar^+, 1–3 keV, 30 min) and annealing until no traces of contaminants could be detected by XPS. The annealing temperatures for Al-Cu-Fe, Al-Pd-Mn, and Al-Ni-Co were, respectively, up to 1023, 923, and 1123 K, leading to a terrace and steps surface termination as checked by STM prior to deposition experiments.

Bi was evaporated from a fully outgassed Knudsen cell. The pressure was kept low (10^{-9} mbar) during deposition. Bi has a rhombohedral structure, which can be considered as a slightly distorted simple-cubic structure. It is only poorly metallic with a low carrier density, and its surface energy is rather low ($\gamma_{Bi}=0.54$ J/m^2).[12]

The deposition flux for a specific setting of the Bi source was estimated from the intensity of the XPS core-level spectra. Specifically, a Bi film of thickness d was deposited on a Pd(111) surface held at room temperature and the intensity of the *Pd* 3*d* core level was monitored as a function of the takeoff angle ϕ (with respect to the surface normal) of the emitted photoelectrons. If I_0 is the intensity of the *Pd* 3*d* signal at the substrate film interface, the measured signal I is to a first approximation $I=I_0e^{-d/\lambda\cos(\phi)}$, where λ is the inelastic mean-free path of the *Pd* 3*d* photoelectrons in the Bi film.

The deposition flux estimated from XPS experiments was crosschecked by analysis of STM images. Bi was deposited at submonolayer coverage on Pd(111) surface, which results in 2D islands. The coverage was then estimated by calculating the area covered by the Bi islands. The flux calculated in this way was close to the value found in XPS measurements. The Bi thin films were characterized using an Omicron room-temperature STM and by RHEED.

III. RESULTS AND DISCUSSION

A. Structure of substrate surface

1. Fivefold surface of i-Al-Cu-Fe and i-Al-Pd-Mn

The structure of *i*-Al-Cu-Fe and *i*-Al-Pd-Mn substrates has already been discussed elsewhere.[13–16] Here, we only provide a brief summary of the main results useful for the understanding of the data presented in this paper. It is observed that the fivefold surface of both samples prepared by sputtering and annealing cycles leads to a terrace and step morphology with atomically smooth terraces extending over several hundreds of nanometers [Figs. 1(a) and 1(c)]. STM reveals steps of different heights: $H=mS+nL$ with (m,n) being consecutive integers of the Fibonacci series, $L\sim0.41$ nm, and $S=L/\tau$, where τ is the golden mean.[15] The analysis of the step-height distribution, within the specific surface preparation explained above, revealed that the most frequent step heights are L, $S+L$, $S+2L$, and $2S+3L$. The occurrence of these steps of, for example, *i*-Al-Cu-Fe is 14%, 32%, 29%, and 15%. The step-height distribution can be explained by bulk truncation at the positions where blocks of atomic layers are separated by larger gaps above regions of relatively dense and high Al content.[17–20]

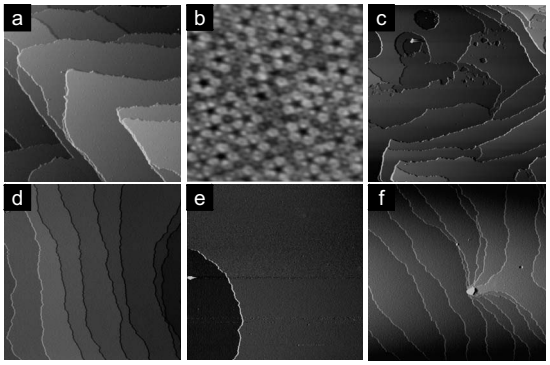

FIG. 1. STM images of the clean fivefold surface of *i*-Al-Cu-Fe (a) 500×500 nm^2 and (b) 10×10 nm^2, *i*-Al-Pd-Mn (c) 1200×1200 nm^2, and the tenfold surface of *d*-Al-Ni-Co (d) 926×926 nm^2, (e) 1000×1000 nm^2, and (f) 500×500 nm^2.

2. Tenfold surface of d-Al-Ni-Co

Compared to the surfaces of icosahedral quasicrystals, the tenfold surface of decagonal quasicrystal is relatively simpler because of existence of periodic order along the surface normal. Terraces are separated by steps of single height of 0.2 nm consistent with the interlayer spacing of the bulk structure. However, details of terrace morphology are sample specific or dependent on surface preparation or the exact composition of the sample (see Ref. 4). The substrate used for this study is *d*-$Al_{71.7}Ni_{18.7}Co_{9.6}$. The sample shows the *S*1-type modification and thus differs from the so-far-investigated Co-rich phases or type-*I* superstructure phases, for which the Co and Ni contents are almost identical.[4]

STM images shown in Figs. 1(d) and 1(e) were taken from the tenfold *d*-$Al_{71.7}Ni_{18.7}Co_{9.6}$ surface prepared at 1023 K. The surface of this phase exhibits fairly large terraces compared to other phases. The typical size of terraces is in the order of 100 nm. However, terraces up to 1 μm wide are also observed occasionally [Fig. 1(e)]. Frequently, we detected small amount of material pining up the steps [Fig. 1(f)]. The reason for this is not clear but we speculate that annealing time during the surface preparation may not be sufficient to allow the diffusion of the material into the terraces. Note that the surface was prepared by flash annealing to avoid the increase in pressure in the UHV chamber during surface preparation. The annealing time used in other studies was generally 0.5–2 h. High-resolution images on terraces exhibit protrusions of atomic height like the surface of other Al-Ni-Co phases (not shown).

B. High-temperature deposition

The growth of Bi at elevated temperature was investigated by using the Al-Cu-Fe substrate. The substrate was held at 523 K during the deposition and observations were performed at room temperature. Figure 2 shows STM images of the surface exposed to approximately 4.5 ML of Bi. The amount of adsorbed Bi estimated from these images is clearly much lower in the submonolayer regime. This is evidenced in Fig. 2(a) where the small Bi islands with bright contrast cover only partially the substrate. The fine structure

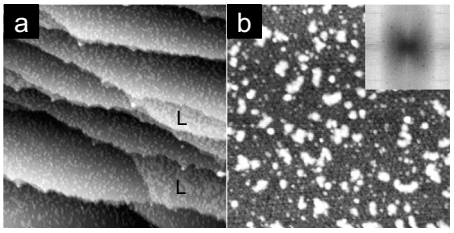

FIG. 2. STM images of the fivefold *i*-Al-Cu-Fe surface after dosing Bi of approximately 4.5 ML at 523 K (a: 300×300 nm^2, b: 70×70 nm^2). The amount of Bi adsorbed on the surface is in submonolayer regime. Inset: Fourier transform of image (inset).

can still be resolved in uncovered area of the quasiperiodic surface. As a result, the fast-Fourier transform (FFT) of the image [Fig. 2(b)] still shows characteristics similar to that of the clean surface with several decagonal rings of spots. The diameters of the rings scale as $1:\tau:\tau^2$, and the decagonal pattern are consistent with the fivefold symmetry of the quasiperiodic substrate. The small amount of adsorbed Bi indicates that the sticking coefficient of Bi on the surface is rather low and/or re-evaporation of Bi adatoms must be easy at 523 K, which is above the multilayer desorption temperature. The Bi islands are approximately 0.2 nm in height. Their lateral size is very limited (a few nanometers) and they are highly irregular in shape. Nevertheless, the aggregation of Bi adatoms into islands indicates that terrace diffusion is activated within the conditions of the deposit.

It is obvious from Fig. 2(a) that the Bi coverage (θ) is not homogeneous over the entire surface but depends on specific terraces. It is possible to estimate θ for a specific terrace from selected area of the STM images. The result of this analysis shows that $\theta\sim25\%-30\%$ on almost every terrace except on those labeled L in Fig. 2(a) where $\theta\sim60\%$. These terraces are bordered by a specific set of step heights. The label L refers to terraces bordered by a 0.66 nm (L+S) step in the uphill direction and by a 0.41 (L) step on top of a 0.66 nm (LS) or (SL) block in the downhill direction. These L terraces account for a limited surface area because L steps represent only 14% of all steps and the L terraces are generally rather small.

Related observations were reported recently by Unal *et al.*[21] for Ag thin films grown on the fivefold surface of *i*-Al-Pd-Mn at 365 K. At submonolayer coverage, it was found that some specific terraces were decorated by a much lower density of Ag islands as compared to other terraces. It is striking that terraces exhibiting this particular behavior for Ag/Al-Pd-Mn are the same specific L terraces presenting a larger coverage compared to other terraces for Bi/Al-Cu-Fe. Three possible explanations for the different island densities were discussed in Ref. 21. The first is terrace width, which can affect island densities due to competition between island nucleation and capture at step edge, as step flow growth can lead to lower island densities on smaller terraces. However, although L terraces are small as noted above, we can always find in STM images terraces of similar size but with a lower Bi coverage. Thus terrace width cannot account for the terrace dependence of the coverage. The second possibility is the Ehrlich-Schwoebel barrier associated with adatom diffu-

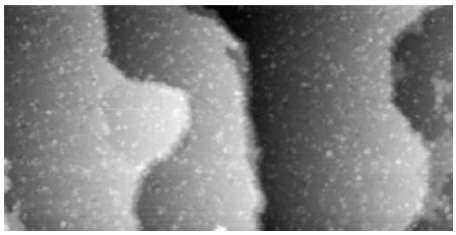

FIG. 3. STM image of the fivefold *i*-Al-Cu-Fe surface covered by a complete monolayer of Bi. The deposition temperature was 523 K (158×80 nm^2).

sion downward a step. In our case, the larger coverage observed on L terraces would suggest that a particle diffusing on this terrace will have to overcome a higher energy barrier for downhill diffusion than on other terraces. However in this case, one should observe a region of increased coverage bordering the downward step, which is in contradiction with the experiment. The third possible explanation relies on the intrinsic nature of the L terraces. Terraces of icosahedral quasicrystals are expected to differ in their exact atomic structures, both in chemistry and atomic densities, which can affect the average distribution of diffusion barrier. In addition, although all terraces are different, they share some common local configurations that appear at different densities. For example the density of the dark stars which has been identified as nucleation sites in a number of studies varies from terrace to terrace in agreement with bulk structure models.[22] Based on rate equation analysis of the experimental data, it was argued that the different island densities observed for Ag/Al-Pd-Mn deposited at 365 K is most likely due to a terrace dependence in the diffusion barrier. In our case, the situation is different because the deposition occurs at much higher temperature (523 K) and desorption of adatoms must be taken into account. If one assumes that the density of trap sites is higher on L terrace, easier nucleation should result in less desorption and higher θ on L terraces.

Another phenomenon that may share some similarities with the present case was reported by Cai *et al.*[23] It concerns the morphology of a 1-ML-thick Al film deposited at room temperature on the same fivefold Al-Cu-Fe surface. It was found that the Al thin film has a lumpy aspect with no well-defined island shape on the vast majority of the terraces except on a few terraces where larger islands with atomically flat tops are observed. As was noted in Ref. 23, these special terraces may correspond to atomic planes containing no nucleation sites identified on other terraces. In this experiment, the coverage was uniform because no evaporation of Al adatoms occurs at room temperature. Sharma *et al.*[24] also reported the observation of terrace-dependent morphology of Sn film deposited on the *i*-Al-Cu-Fe surface.

Figure 3 shows an STM image of the surface covered by a complete Bi monolayer on the fivefold *i*-Al-Cu-Fe. In this case, the deposition time was long enough to produce the expected Bi monolayer, and the deposition temperature was high enough to achieve (almost) complete desorption of Bi multilayer. Therefore the film is relatively smooth and the terrace and step morphology of the substrate are not modified by the film. However, the roughness on the terraces is still

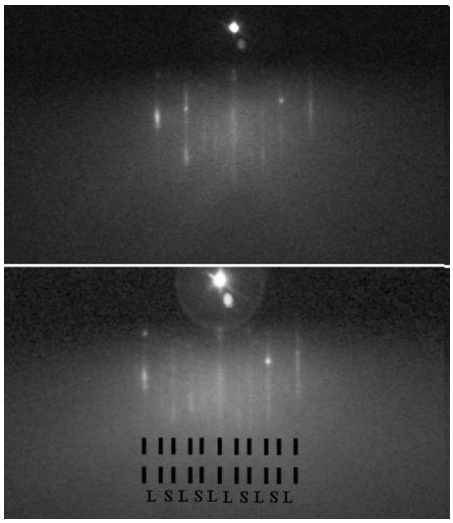

FIG. 4. RHEED patterns from the clean fivefold surface of *i*-Al-Cu-Fe (a) and the same surface after the deposition of a complete monolayer (b).

larger for the clean substrate mainly due to the remaining small amount of adatoms on top of the monolayer appearing as white dots in Fig. 3. This increased roughness is detrimental to the STM resolution and we could not obtain information on the atomic structure of the Bi monolayer. Annealing of the Bi monolayer could be used in later studies to improve its structural quality, as demonstrated in the recent studies of quasiperiodic Pb monolayers formed on the fivefold *i*-Al-Pd-Mn surface.[25] Figure 4 shows a RHEED pattern obtained either before or after the formation of the Bi wetting layer. Both diffraction patterns are characteristic of a quasicrystalline surface with streaks separated by long (L) and short (S) spacing with $L/S \sim \tau$. This result does not prove unambiguously that the Bi monolayer has adopted the quasiperiodic substrate structure (because the thickness probed by RHEED is typically several nanometers, i.e., much larger than the film thickness). It is consistent with previous observation by HAS reported by Franke *et al.*[6] demonstrating the quasiperiodic nature of the Bi monolayer formed on the isostructural fivefold surface of *i*-Al-Pd-Mn. Finally we mention the recent report by Smerdon *et al.*[26] demonstrating the quasiperiodic structure of a similar Bi monolayer grown on the fivefold surface of *i*-Al-Pd-Mn by STM.

C. Room-temperature deposition

1. i-Al-Cu-Fe substrate

a. Growth of a quasiperiodic monolayer. By depositing Bi at lower substrate temperature, one expects a reduced probability for the re-evaporation of adatoms as well as reduced adatom mobility. The STM image in Fig. 5(a) encompasses one single terrace of the surface dosed with approximately 0.35 ML of Bi. The coverage estimated from such images is about a third of a monolayer, which is very close to the deposited amount. Therefore the sticking coefficient of Bi on the quasicrystalline surface is close to unity at room temperature, and re-evaporation of adatoms is inhibited as

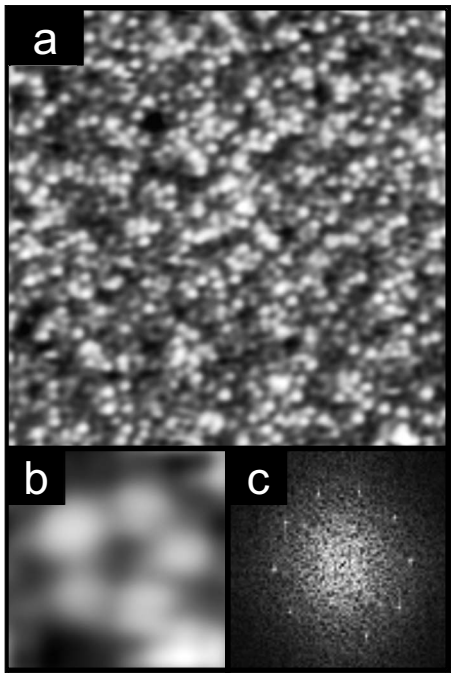

FIG. 5. (a) STM topography (30×30 nm^2) of the fivefold $Al_{63}Cu_{24}Fe_{13}$ surface dosed with 0.35 ML of Bi. (b) Local pentagonal motif formed by five Bi adatoms (2.5×2.5 nm^2). (c) FFT of the image in (a).

expected. The film morphology is significantly different from that in Fig. 2(b). There is no island formation and dots of bright contrast in Fig. 5 must correspond to a single Bi adatom. As expected, terrace diffusion is not activated at room temperature in the submonolayer regime. Height profiles taken across Bi adatoms give a value of about 0.15 nm, which is significantly smaller than the island height measured for high-temperature growth (0.2 nm). This effect must result from a different Bi-substrate bonding depending on whether the Bi adatoms is isolated or embedded in an island.

At this submonolayer coverage, the fine structure of the quasiperiodic substrate can still be resolved. As a result, the FFT of the STM images is a tenfold symmetric pattern [Fig. 5(c)]. FFT of STM image, obtained by applying an appropriate height threshold to select the Bi adatoms, also demonstrates the tenfold symmetric arrangement of the adatoms. This as well as the observation of local fivefold configuration of Bi adatoms [Fig. 5(b)] is consistent with a quasiperiodic growth of the first Bi monolayer.

b. Nanocrystallites and rotational epitaxy. For coverage larger than one monolayer, once the first Bi wetting layer has been completed, we observe the formation of islands. Figures 6(a)–6(c) shows an STM image of the surface exposed to 4.5 ML of Bi. Most of the islands have sharp edges and smooth tops. The RHEED pattern of the Bi film is shown in Fig. 6(d). The pattern consists of diffraction spots (not streaks) aligned along straight lines, indicating transmission-reflection diffraction through the 3D Bi islands. The distribution of spots shows that the film grows with a pseudocubic (100) orientation, which is equivalent to (012) in the rhombohedral system.[27] The small-spot size also shows the good crystallinity of the islands. Our system allows for *in situ* azimuthal rotation around the surface normal and it is observed that the same diffraction pattern appears every 72°. This demonstrates that the epitaxial relationship within the surface plane is defined by the alignment of a crystallographic axis of the Bi islands with one of five equivalent directions within the Bi wetting layer. The fivefold twinning of the Bi crystallites can also be deduced from angles between step edges of adjacent Bi islands, which are multiples of $\pi/10$, consistent with the fivefold rotational symmetry of the first Bi layer.

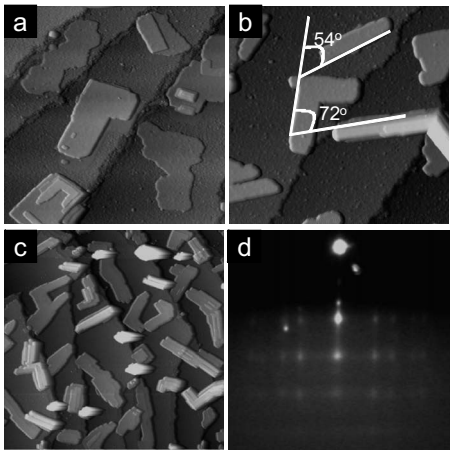

FIG. 6. (a)–(c) STM images of the fivefold surface of *i*-Al-Cu-Fe after deposition of about 4.5 ML of Bi at room temperature: (a) 150×150 nm^2, (b) 185×185 nm^2, and (c) 500×500 nm^2. (d) RHEED pattern from the same surface.

c. Magic heights. Most interesting is the fact that the Bi crystallites have a specific height of ~1.3 nm or a multiple of this height. In a few cases, islands with approximately half of this height could also be observed but never one-layer-thick islands. These islands are of irregular shape and are only observed immediately after the deposition, but they disappeared with time. In the rhombohedral system, the interlayer spacing along the [012] direction is $d_{012}=0.328$ nm and therefore we conclude that the vast majority of islands has a thickness corresponding to the stacking of four atomic layers in the (012) orientation or a multiple of this height. The occurrence of magic island heights reveals a special stability for certain thickness, which we are going to discuss in Sec. III C 4.

2. i-Al-Pd-Mn substrate

Figure 7 shows the *i*-Al-Pd-Mn surface after Bi deposition at 1.02 and 4.5 ML, which covers the amount of Bi occupied by islands and the underneath Bi wetting layer. The growth mode of Bi on this substrate is similar to that observed on the *i*-Al-Cu-Fe substrate. For both coverage, the deposited Bi forms islands corresponding to the stacking of four (012) layers (4L islands) or a multiple of this height. The bilayer islands were also observed at early stages of the growth but again they disappeared afterward. Similarly, the islands grow

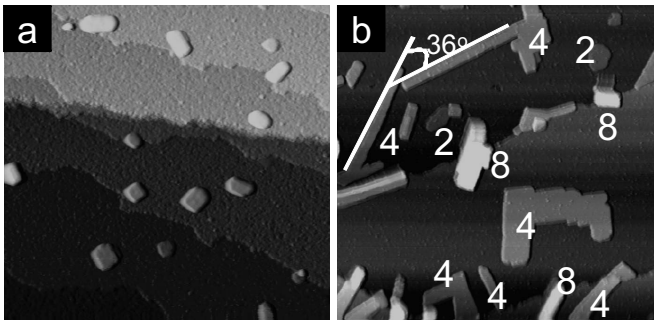

FIG. 7. STM images of the fivefold surface of *i* -Al-Pd-Mn after deposition of (a) 1.02 ML (150×150 nm^2) and 4.5 ML (400×400 nm^2) of Bi at room temperature. The height of the islands in ML units is indicated in (b).

with the [012] rhombohedral axis (i.e., pseudocubic [100] axis) being parallel to the surface normal. Within the surface plane, islands have five different possible orientations with respect to the substrate rotated by angles of $n\pi/10$ from each others. Furthermore, the stability of islands was investigated by annealing the surface at different temperatures, which will be described in Sec. III C 5.

3. d-Al-Ni-Co substrate

a. Coverage-dependent growth mode. The *d*-Al-Ni-Co substrate was used to investigate the growth of Bi at wider coverage ranges. STM images from the surface for different coverage up to 10 ML are shown in Fig. 8. Three different growth modes are observed depending on θ. For $\theta\leq1$, a smooth growth is observed as shown in Fig. 8(a). The Fourier transform of the image shows tenfold symmetry and τ scaling relationships [Fig. 8(a) inset] suggesting again a quasiperiodic structure of the first wetting layer. For $1<\theta<5$, islands are formed. The height of almost all islands is 1.26 nm ($\sigma=0.03$), corresponding to 4L islands with (012) orientation. In rare cases, 8L islands were also observed. These results are consistent with those observed on the *i*-Al-Cu-Fe and *i*-Al-Pd-Mn surfaces. For increasing coverage, the islands predominantly grow laterally.

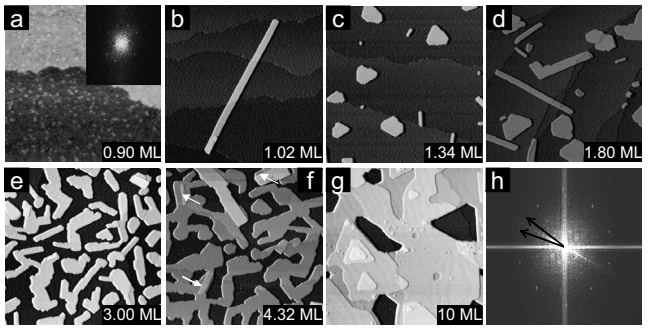

FIG. 8. (a)–(g) STM images of the tenfold surface of *d*-Al-Ni-Co after deposition of Bi at different coverage at room temperature: (a) 80×80 nm^2; inset: Fourier transform of the image, (b) 300×300 nm^2, (c) 400×400 nm^2, (d) 300×300 nm^2, (e) 250×250 nm^2, (f) 250×250 nm^2, and (g) 200×200 nm^2. (h) Fourier transform of image (b).

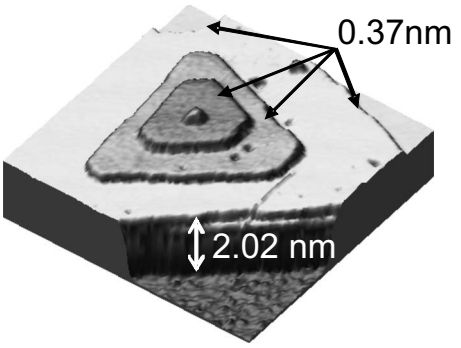

FIG. 9. A section of STM image in Fig. 8(g) in a 3D view (68×68 nm^2).

Above 5 ML, Bi grows with monatomic step height. Indications of an early stage of this third growth mode are apparent already for $\theta=4.3$ ML as monatomic steps already appears [marked by arrows in Fig. 8(f)]. Figure 9 shows a 3D view of an STM image for 10 ML coverage showing a pyramidlike island with triangular shape on top of a smooth film. The step height measured on triangular islands is 0.37 nm ($\sigma=0.01$), which is close the interlayer spacing $d_{001}=0.39$ nm in the rhombohedral notation. RHEED patterns from the surface confirm the (001) surface orientation of the film at this stage (Fig. 10). The change from the (012) to the (001) orientation was also observed for Bi growth on the Si(111) substrate.[27] The triangular symmetry is expected from the bulk Bi.[27] These triangular islands have different in-plane orientations rotated by $n\pi/10$ with each other. This results from the fivefold twinning of the Bi domains with (012) orientation on which the growth started. As a consequence, grain boundaries can be observed on STM images

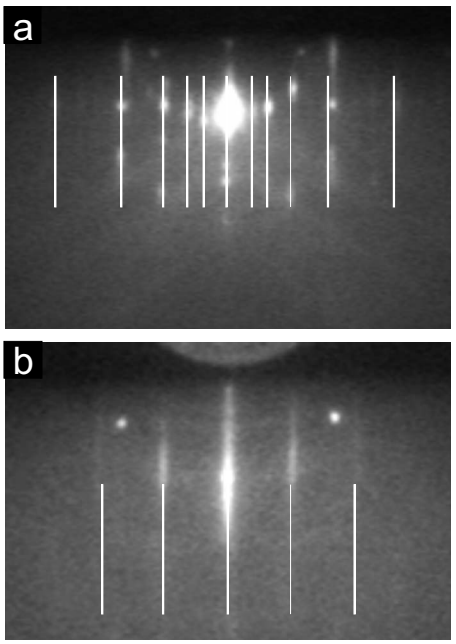

FIG. 10. RHEED patterns from the tenfold surface of *d*-Al-Ni-Co. (a) Clean surface and (b) after the deposition of 10 ML Bi.

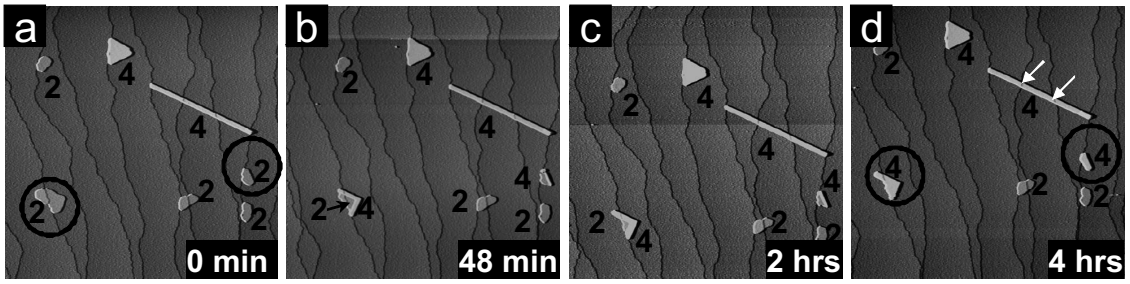

FIG. 11. STM images recorded at different time intervals (given) from a certain place of the tenfold *d*-Al-Ni-Co surface after the deposition of 1.02 ML Bi (700×700 nm^2). The height of the islands is given. White arrows in (d) indicate step edges of Bi islands.

separating adjacent domains with different orientations.

b. Evolution of islands with magic heights. In our experimental systems, the deposition of Bi and the STM measurements were carried out in two different chambers. Therefore, it was not possible to monitor the growth of the Bi film simultaneously during deposition. In order to observe the early stage of the growth, we minimized the time between deposition and the first acquisition of STM images down to 10 min (compared to an hour or more for previous experiments on *i*-Al-Cu-Fe and *i*-Al-Pd-Mn). Just after deposition, a high density of two atomic height islands could be observed. The precise height estimated from a large number of 2L islands is found to be 0.68 nm. The expected height of the 4L islands should thus be equal to 1.36 nm, which is significantly larger than their measured height (1.26 nm) using the same tunneling parameters. The evolution of the film morphology into 4L islands could be followed by recording STM images of the same area over several hours. We found that two different processes occur. The 2L islands either reshaped themselves into 4L islands or they coalesce with neighboring 4L islands as described below.

Figures 11(a)–11(d) show STM images after the deposition of 1.02 ML and recorded at the same place with same tunneling parameters but at different times (given in the figure). We collected 50 images in 4 h. The images recorded at selected time intervals are given in the figure. As previously observed for Bi on *i*-Al-Cu-Fe or *i*-Al-Pd-Mn surfaces, 2L islands are irregular in shape, whereas 4L islands are highly faceted. As can be seen, the shape of the 4L islands remain unchanged in the given measurement time, but the 2L islands (marked by circles in the figure) gradually rearrange themselves. There is a mass transportation within the islands in order to reorder themselves into 4L islands with highly oriented edges.

Islands are often embedded at step edges of the substrate, suggesting easy diffusion of Bi adatoms on the wetting layer and preferential nucleation at step edges. Sometimes, islands extend over step edges [indicated by arrows in Fig. 11(d)] and the step height on the islands reproduces the step height of the substrate.

The coalescence of islands is illustrated in Fig. 12 showing a sequence of STM images recorded on the same area of a single terrace after the deposition of 1.34 ML on a freshly prepared surface. Again, we can identify two types of islands: elongated 4L islands and irregularly shaped 2L islands. It is obvious that Bi atoms diffuse from 2L islands to 4L islands resulting in larger 4L islands and a lower density of 2L islands with time. Interestingly, Bi atoms tend to attach preferentially at the end of the islands rather than at the sides, and therefore the islands grow anisotropically. As noted above, the diffusion of Bi adatoms on the wetting layer is easy, contrasting with the reduced mobility on the clean surface (as explained in Sec. III C 1). This is consistent with earlier observation by He-atom scattering revealing the inertness of the wetting layer.[6]

We found that the 2L islands have completely disappeared from all part of the surface several hours after the deposition. An example of such STM images is shown in Fig. 8(c). The few islands with lumpy aspects observed at the early state of the growth (middle left right part of Fig. 12) also disappeared after this time.

c. Growth direction. As explained in Sec. III C 3 b, the growth of 4L islands is anisotropic. The growth direction can be determined with respect to the substrate high-symmetry

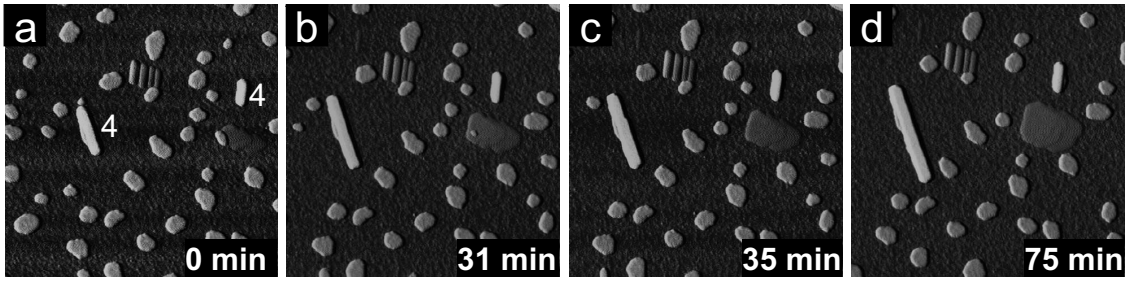

FIG. 12. STM images recorded at different time interval (given) from a single terrace of the tenfold *d*-Al-Ni-Co surface after the deposition of 1.34 ML Bi (170×170 nm^2).

axes by analyzing Fourier transform of STM images. The Fourier transform of the STM image given in Fig. 8(b), which was obtained at 1.02 ML coverage, is shown in Fig. 8(h). This shows two distinct features: rings of bright spots and a slit, which is perpendicular to the Bi rod. The spots result from the structure of the wetting layer while the slit is related to the Bi rod. The two rings of spots have τ scaling relationship and exhibit tenfold symmetry. This further confirms that the wetting layer underneath the islands is quasiperiodic.

The substrate comprises two nonequivalent set of twofold axes. In the Fourier transform, the directions along the brightest spots from the center correspond to one set of the twofold axes, while another set is rotated by 18° with respect to this set. Representative of these axes is indicted by arrows in the Fourier transform image. The slit is rotated by 9° from these high-symmetry axes of the substrate. This reveals that growth direction of the Bi islands is not along the twofold axes of the substrate but in between them. The high-symmetry axes of the bulk Bi in the islands could not be determined because our attempts to resolve atomic structure of the islands by STM were unsuccessful.

4. Interpretation of magic heights

The interpretation of the special stability associated with specific film thicknesses or island heights relies on QSE. As the thickness of a film is reduced to the nanometer scale, the confinement of the electron at the film/substrate and film/vacuum interfaces leads to the formation of discrete electronic states (quantum well states). Because the energy of the quantum well states depends on the film thickness t, the physical properties of the film also vary with t. This is true also for the film stability because the electronic contribution to the total energy of the film depends on t. As a result, films or islands of specific thicknesses can have an enhanced stability over other thicknesses due to QSEs. The existence of quantum well states close to the Fermi level will enhance the DOS at the Fermi level, increasing the electronic contribution to the total energy of the film. Preferred films or islands thicknesses with enhanced stability are those for which the energies of the quantum well states are well below the Fermi level. The occurrence of specific island height selection has been reported not only in several metal thin films grown on semiconductor substrates such as Ag, Pb, and Bi on Si(111) (Refs. 27–29) or Ag on GaAs (110) (Ref. 30) but also in metal heterostructures such as Pb on Cu(111) (Ref. 31) or Ag on Fe(100).[32] For recent review on QSE in metallic thin films with more examples, see Refs. 33 and 34.

In our earlier report, we interpreted the occurrence of magic island heights observed on Ag/Al-Pd-Mn and Bi/Al-Cu-Fe as a manifestation of QSE. We hypothesized that the origin of the confinement at the film/substrate interface could be due to the reduced density of states at the Fermi characteristic of these alloys. Later, Moras *et al.*[11] directly observed by photoemission spectroscopy the quantum well states in Ag thin films deposited on either the fivefold surface of *i*-Al-Pd-Mn or the tenfold surface of *d*-Al-Ni-Co, thus confirming the suggested electronic growth mechanism. However, it was found that these quantum well states did not display any dependence on the density of states of the quasicrystalline substrates, which are significantly different for both substrates. It was therefore concluded that the confinement may be driven by the incompatible symmetries of the electronic states of the crystalline film and the quasicrystalline substrate. Our observations of a height selection mechanism in the case of Bi deposited on three different systems shows that QSE appears to be rather general on quasiperiodic substrates independent of their detailed electronic structure. We mentioned earlier that the height of the unstable 2L islands on Al-Ni-Co substrate measured by STM is significantly larger than half of the value for the 4L islands. This is consistent with a larger local density of states in the vicinity of the Fermi level for 2L islands compared to 4L islands. Therefore the driven force for the islands to reshape into 4L islands would be to lower $N(E_F)$ and thus the electronic energy of the system.

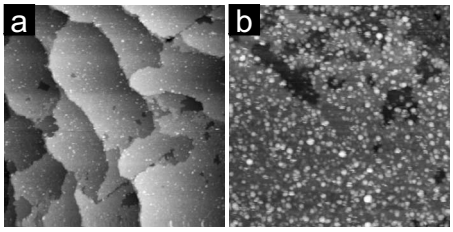

FIG. 13. STM images of the fivefold *i*-Al-Pd-Mn surface after the deposition of 4.5 ML Bi and annealing at 623 K. (a) 300×300 nm^2 and (b) 133×133 nm^2.

5. Thermal stability of the islands with magic heights

The stability of the Bi islands was examined by annealing the 4.5-ML-thick Bi film (Fig. 7) at different temperatures up to 623 K. The XPS spectra taken from the surface during annealing suggest that Bi starts desorbing above room temperature. However, a significant amount of Bi was still detected after annealing the surface at 623 K. The sample was then cooled down to room temperature and the surface was imaged by STM. As seen in Fig. 13, the Bi islands completely desorbed and the first layer remains. The desorption of the islands was expected because the employed temperature was above the multilayer desorption temperature of 523 K found by He-atom scattering data.[6]

A part of motivation of our annealing experiments was to obtain a monolayer of Bi by desorbing atop islands and to resolve atomic structure by STM. However, the film obtained after annealing was found rougher than the monolayer obtained by direct deposition on the *i*-Al-Pd-Mn surface at elevated temperature (Sec. III B) or on the *d*-Al-Ni-Co surface at room temperature (Sec. III C 3), making it difficult to get atomically resolved STM images. The film obtained after desorbing the islands can be seen in a magnified view in Fig. 13(b). The RMS roughness is 0.2 nm.

6. Comparison with Bi growth on Si(111)

Previous studies by STM and *ab initio* have shown that Bi growth on Si(111) also yields islands of magic heights.[27,35]

However, our results show the following features distinct from these reports. First, these studies found that even number layer films are prominently stable, where 2L islands are expected to be the most stable. The mechanism that induces even number layer films was ascribed to large atomic relaxation, which paired each two neighboring layers and avoids dangling bonds.[27] However, we clearly observe that the 2L islands are unstable in our case. They either reshape into 4L islands or coalesce to the neighboring 4L islands (Sec. III C 3 b). Second, the model predicted that the pairing of the layers occurs independently from the nature of the substrate. However, we deposited Bi on the Pd(111) surface and found no evidence of magic thicknesses or layer pairing effect. Therefore, we believe that the origin of the magic height thickness on quasicrystal surfaces is not the pairing effect but rather the quantum size effect as described in Sec. III C 4.

IV. SUMMARY AND CONCLUSION

We investigated the growth of Bi on three different quasicrystal surfaces at two different growth temperatures 300 and 525 K and at different coverage from submonolayer to 10 ML. The substrates were the fivefold *i*-Al-Cu-Fe and *i*-Al-Pd-Mn surfaces and the tenfold *d*-Al-Ni-Co surface. We combined various techniques including STM, RHEED, and XPS to characterize the growth. A wide variety of structures were observed depending on experimental conditions. This includes quasiperiodic Bi layer, nanocrystallites of magic heights, rotational epitaxial relation of the film with the substrate, and terrace-dependent film morphologies.

At 300 K, three different growth modes were observed depending on θ. For $\theta \leq 1$, it grows smoothly forming a quasiperiodic layer. For $1 < \theta < 5$, nanoislands with (100) surface orientation are formed. The islands have magic height of four atomic layer (predominantly). The islands are aligned along certain directions of the substrates resulting in twinning structures with the symmetry of the substrate. The islands predominantly grow laterally with increasing coverage and form almost a complete layer of four atomic height. For higher coverage, it grows with monatomic height, not with magic height, and reflects triangular symmetry expected from the bulk Bi.

We were able to monitor the growth of islands with respect to time by depositing Bi at converge slightly above 1 ML and measuring STM images of the same area in several-minute intervals over several hours. We found that the four-layer islands are most stable. The two-layer islands observed immediately after deposition either reshaped themselves into four-atom-high islands or coalesced with neighboring four-layer islands. The selection of four atomic height is ascribed to quantum size effects, arising from the confinement of the electron within the film, which is manifested by the electronic structure of the quasicrystalline substrates.

At 525 K, only the first layer can be adsorbed, not the multilayers. This temperature is enough to activate terrace diffusion resulting in the aggregation of Bi adatoms and yielding a smooth layer of quasiperiodic order at monolayer coverage. At submonolayer coverage, the amount of Bi observed on different terraces is found to be different, which is explained in terms of re-evaporation of Bi from selective terraces.

ACKNOWLEDGMENT

H.R.S. is grateful to EPSRC for funding (Grant No. EP/D071828/1).

*Corresponding author. Present address: Department of Physics, The University of Liverpool, Liverpool L69 3BX, UK; h.r.sharma@liv.ac.uk

[1] D. Shechtman, I. Blech, D. Gratias, and J. W. Cahn, Phys. Rev. Lett. **53**, 1951 (1984).
[2] Z. M. Stadnik, *Physical Properties of Quasicrystals* (Springer, New York, 1999).
[3] G. Trambly de Laissardiere, D. Nguyen-Manh, and D. Mayou, Prog. Mater. Sci. **50**, 679 (2005).
[4] H. R. Sharma, M. Shimoda, and A. P. Tsai, Adv. Phys. **56**, 403 (2007).
[5] V. Fournee and P. A. Thiel, J. Phys. D **38**, R83 (2005).
[6] K. J. Franke, H. R. Sharma, W. Theis, P. Gille, Ph. Ebert, and K. H. Rieder, Phys. Rev. Lett. **89**, 156104 (2002).
[7] M. Krajci and J. Hafner, Phys. Rev. B **71**, 184207 (2005).
[8] M. Krajci and J. Hafner, Phys. Rev. B **73**, 184202 (2006).
[9] V. Fournée, H. R. Sharma, M. Shimoda, A. P. Tsai, B. Unal, A. R. Ross, T. A. Lograsso, and P. A. Thiel, Phys. Rev. Lett. **95**, 155504 (2005).
[10] H. R. Sharma, M. Shimoda, and A. P. Tsai, Jpn. J. Appl. Phys., Part 1 **45**, 2208 (2006).
[11] P. Moras, Y. Weisskopf, J.-N. Longchamp, M. Erbudak, P. H. Zhou, L. Ferrari, and C. Carbone, Phys. Rev. B **74**, 121405(R) (2006).
[12] L. Vitos, A. V. Ruban, H. L. Skriver, and J. Kollar, Surf. Sci. **411**, 186 (1998).
[13] M. Gierer, M. A. Van Hove, A. I. Goldman, Z. Shen, S.-L. Chang, P. J. Pinhero, C. J. Jenks, J. W. Anderegg, C.-M. Zhang, and P. A. Thiel, Phys. Rev. B **57**, 7628 (1998).
[14] Z. Papadopolos, G. Kasner, J. Ledieu, E. J. Cox, N. V. Richardson, Q. Chen, R. D. Diehl, T. A. Lograsso, A. R. Ross, and R. McGrath, Phys. Rev. B **66**, 184207 (2002).
[15] H. R. Sharma, V. Fournée, M. Shimoda, A. R. Ross, T. A. Lograsso, A. P. Tsai, and A. Yamamoto, Phys. Rev. Lett. **93**, 165502 (2004).
[16] T. Cai, V. Fournée, T. Lograsso, A. Ross, and P. A. Thiel, Phys. Rev. B **65**, 140202 (2002).
[17] A. Yamamoto, H. Takakura, and A. P. Tsai, Phys. Rev. B **58**, 094201 (2003).
[18] A. Yamamoto, H. Takakura, and A. P. Tsai, J. Alloys Compd. **342**, 159 (2002).
[19] A. Yamamoto, H. Takakura, and A. P. Tsai, Ferroelectrics **305**, 279 (2004).
[20] H. Takakura, A. Yamamoto, and A. P. Tsai, Acta Crystallogr.,

Sect. A: Found. Crystallogr. **57**, 576 (2001).
[21] B. Unal, J. W. Evans, T. A. Lograsso, A. R. Ross, C. J. Jenks, and P. A. Thiel, Philos. Mag. **87**, 2995 (2007).
[22] J. Ledieu and R. McGrath, J. Phys.: Condens. Matter **15**, S3113 (2003).
[23] T. Cai, J. Ledieu, R. McGrath, V. Fournee, T. Lograsso, A. Ross, and P. Thiel, Surf. Sci. **526**, 115 (2003).
[24] H. R. Sharma, M. Shimoda, A. R. Ross, T. A. Lograsso, and A. P. Tsai, Philos. Mag. **86**, 807 (2006).
[25] J. Ledieu, L. Leung, L. H. Wearing, R. McGrath, T. A. Lograsso, D. Wu, and V. Fournée, Phys. Rev. B **77**, 073409 (2008).
[26] J. Smerdon, J. Parle, L. Wearing, T. A. Lograsso, A. R. Ross, and R. McGrath, Phys. Rev. B **78**, 075407 (2008).
[27] T. Nagao, J. T. Sadowski, M. Saito, S. Yaginuma, Y. Fujikawa, T. Kogure, T. Ohno, Y. Hasegawa, S. Hasegawa, and T. Sakurai, Phys. Rev. Lett. **93**, 105501 (2004).
[28] L. Huang, S. J. Chey, and J. H. Weaver, Surf. Sci. **416**, L1101 (1998).
[29] V. Yeh, L. Berbil-Bautista, C. Z. Wang, K. M. Ho, and M. C. Tringides, Phys. Rev. Lett. **85**, 5158 (2000).
[30] D. A. Evans, M. Alonso, R. Cimino, and K. Horn, Phys. Rev. Lett. **70**, 3483 (1993).
[31] R. Otero, A. Vasquez de Parga, and R. Miranda, Phys. Rev. B **66**, 115401 (2002).
[32] D.-A. Luh, T. Miller, J. J. Paggel, M. Y. Chou, and T.-C. Chiang, Science **292**, 1131 (2001).
[33] T.-C. Chiang, Surf. Sci. Rep. **39**, 181 (2000).
[34] M. Milun, P. Pervan, and D. P. Woodruff, Rep. Prog. Phys. **65**, 99 (2002).
[35] M. Saito, T. Ohno, and T. Miyasaki, Appl. Surf. Sci. **237**, 80 (2004).